Proceedings World Geothermal Congress 2005
Antalya, Turkey, 24-29 April 2005

# Geothermal Reservoir Characterization by SP Monitoring

Kasumi Yasukawa[1], Tsuneo Ishido[1] and Tatsuya Kajiwara[2]

[1]Geological Survey of Japan (AIST), AIST Tsukuba Central 7, Tsukuba, Ibaraki, 305-8567, Japan

[2]JMC Geothermal Engineering Co., LTD, 1-101 Hosoyachi, Ukai, Takizawa, Iwate-gun, Iwate, 020-0172, Japan

kasumi-yasukawa@aist.go.jp

**Keywords:** self-potential, resistivity, hydrothermal system, monitoring, geothermal reservoir, Nigorikawa, Mori, Matsukawa, Japan

## ABSTRACT

Self-potential (SP) method is applied for monitoring of both liquid dominated and steam dominated geothermal systems. Practical procedures of SP monitoring data analyses are discussed with simulation results and field data from Mori liquid dominated geothermal system. As a preliminary study for a steam dominated system, repeat SP survey at the Matsukawa geothermal system was conducted. The result shows that SP monitoring allows us to realize the hydrological characteristic of each observation point for both steam dominated and water dominated reservoirs.

## 1. INTRODUCTION

Self-potential (SP) measurements have been conducted for geothermal field exploration and, recently, also for reservoir monitoring assuming that the main cause of the SP anomaly is streaming potential. Several authors have been reported the change of SP distribution after fluid production at liquid dominated geothermal reservoirs, such as Cerro Prieto (Goldstein et al., 1989), Mexico, Mori (Ishido and Pritchett, 2000), Sumikawa (Matsushima et al., 2000), and Yanaizu-Nishiyama, Japan (Tosha et al., 2000), etc. The application of continuous SP measurement on reservoir monitoring has been studied for Hachijojima (Nishino et al., 2000) and Mori (Yasukawa et al., 2001).

One of the difficulties in interpretation of continuous SP data is that there are many causes which perturb the surface SP such as artificial noises, magnetic field perturbation caused by solar activity, rainfall effect, etc. Therefore it is difficult to identify the SP change caused by the subsurface fluid flow. Another problem is that it is almost impossible to find a reference point in the field where electric potential is constant so that the SP at each monitoring point can be recorded in comparison to this point. Therefore a problem of setting base point is always an obstacle for SP monitoring.

This paper introduces the concept of "relative" SP observation. "Relative" SP proposed in this paper is obtained assuming that the average SP among monitoring points at each moment is always zero. In the next section, advantages of "relative" SP will be shown through simulation results. Then the following section shows the results of continuous SP observations conducted in the Nigorikawa basin, Hokkaido, where Mori geothermal power plant is in operation since 1982. As results, change of relative SP during well operations reflects the hydro-geological characteristics of the reservoir and each monitoring point.

This paper also presents the possibility of SP monitoring for vapor dominated geothermal reservoirs. It might be difficult to identify the changes of SP caused by reservoir operations at steam reservoirs due to the fact that the streaming potential for steam is almost zero. Nevertheless, existence of slight liquid water may allow SP observations to detect the movement and/or the phase change of the reservoir fluid. Therefore the authors conducted repeat SP observations at the Matsukawa geothermal field, Iwate, Japan where geothermal steam has been produced for power station since 1966. In 2002, surface SP distribution was widely measured three times before and after shut-in of the wells for annual maintenance. The result shows the change of SP around the major production zones. The possible mechanism of SP change for vapor-dominated reservoirs will be discussed in this paper.

## 2. ADVANTAGES OF "RELATIVE" SELF-POTENTIAL OBSERVATION

Relative SP is obtained as differential from the average of all observed SP values at each moment. Relative SP at n-th observation point Vr (n) can be expressed as;

$$V_r(n) = V(n) - \left(\sum_{i=1}^{N} V(i)\right) / N \qquad (1)$$

where V(n), n=1,N is the observed SP at n-th observation point in refer to a certain reference point. This statistical method is useful to characterize the behavior of each observation point because it is difficult to find a stable reference point. Since the mutual characteristic of each point is emphasized in relative SP method, it has an advantage even in an ideal case in which there is no SP perturbation at a reference point. This advantage will be proven in this section through simulation results calculated with a coupled fluid-flow and SP simulation code PTSP (Yasukawa et al, 1993).

### 2.1 Theoretical background of the numerical simulation

The total electrical current flow per unit area J (A/m2) caused by electric and hydraulic gradients may be described as (Mitchell, 1993):

$$\mathbf{J} = -L_v\mathbf{u} + \sigma\mathbf{E} \qquad (2)$$

where $L_v$ is the velocity cross-coupling conductivity (A-s/m$^3$), $\mathbf{u}$ is the velocity field (m/s), $\sigma$ is the electrical conductivity (S/m) and $\mathbf{E} = -\nabla\Phi$ is the electric field (V/m). For details, see Yasukawa et al. (2003). In a medium where there are no external current sources such as current electrodes, the divergence of the total current is zero; $\nabla\cdot\mathbf{J} = 0$. Taking the divergence of equation (2) this current S (A/m$^3$) caused by fluid flow can be expressed as:

$$S = \nabla\cdot\sigma\mathbf{E} = -\nabla L_v\cdot\mathbf{u} - L_v\nabla\cdot\mathbf{u} \qquad (3)$$

For a given velocity field, equation (3) allows us to calculate the electrical potential source at each point.

According to Sill (1982), the variation of $L_v$ with temperature T below 300˚C is approximately described by:

$$L_v(T) = L_{v_0}(1+C\Delta T) \quad \Delta T = T - T_0 \qquad (4)$$

where C is a constant and subscript 0 indicates the reference temperature $T_0$. This equation is introduced into PTSP with the constant C =0.01 (˚$C^{-1}$), which is consistent with the experimental results of Ishido and Mizutani (1981) and Morrison et al. (1978), and analytical equations derived by Revil et al. (1999).

For calculation by PTSP, first we need input data on hydro-thermodynamic rock parameters including permeability. Temperature and pressure changes in a system are simulated on the basis of the energy and mass conservation equations for proper initial and boundary conditions. We thus obtain the distribution of fluid velocity and calculate the potential source distribution caused by fluid flow with equation (3). The related SP distribution is then calculated for a given resistivity and the cross-coupling conductivity structure.

### 2.2 Numerical simulation of fluid production and injection

Fig. 1 shows a 2D reservoir model. Before production and injection begin, the system has reached a steady state with a constant homogeneous surface temperature of 20˚C and pressure of 1 atm. Hot fluid sources of 260˚C are assumed at the bottom of high permeability reservoir. The right and left bottom grid blocks are constant at 150˚C. Rock porosity is 0.2 for all grid blocks. The other rock parameters of each grid block, such as permeability, electric resistivity and cross-coupling conductivity, are shown in Fig. 1. Resistivity values are representative values for Mori geothermal field (Kajiwara et al., 1995), while cross-coupling conductivity values are arbitrarily set in a range of proper ones for volcanics (Yasukawa et al., 2003).

Production and injection begins at time $t$ = 0 and stops at a year later. Seventy-five percent of the produced fluid is injected from a shallower part of the reservoir at 80˚C with flow rates shown in Fig.1. Then the change of SP at ground surface is simulated by PTSP. The number of the supposed SP observation points is 25 as shown in Fig.1.

Fig. 2 shows the simulated change of absolute SP, which is obtained with a reference point in infinity. Fig. 3 shows the simulated absolute SP profiles from $t$ = 0 to 1 month after production stops

Since the effect of injection is dominant to that of production because of its shallower positioning, absolute SP decreases at all observation points over the reservoir range. Similar results are obtained with a reference point at the edge of the observation range, *i.e.*, at $x$ = -1.0 or 1.5 km.

Fig. 4 shows the change of “relative” SP for the same case. Around the production zone (left side of Fig. 1, shown as $x$ = -900, -600, -300 and 0 m in Fig. 4), relative SP increases with production while it decreases around the injection zone (right side of Fig. 1, $x$ = 300, 600, 900 m). Fig. 5 shows relative SP profiles. Different behaviors of production and injection zones are clearly indicated also in Fig. 5.Since the effect of injection is dominant to that of production because of its shallower positioning, absolute SP decreases at all observation points over the reservoir range. Similar results are obtained with a reference point at the edge of the observation range, *i.e.*, at $x$ = -1.0 or 1.5 km.

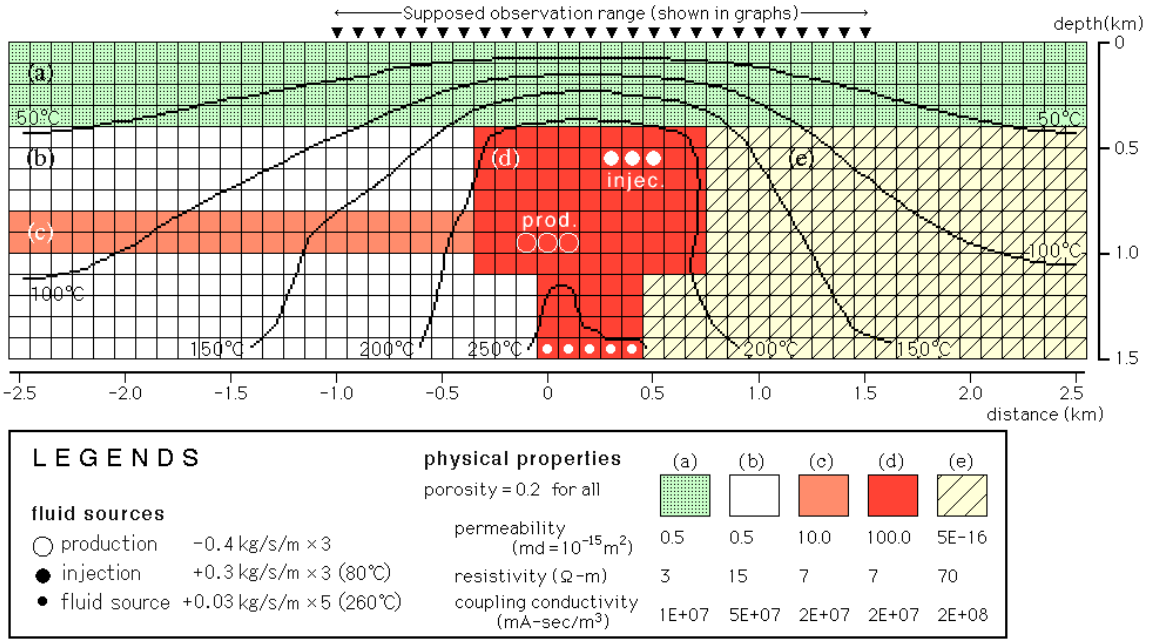


**Fig. 1 Reservoir model**

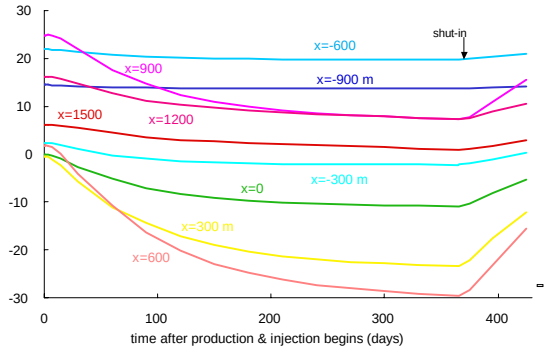


**Fig. 2 Simulated change of absolute SP.**

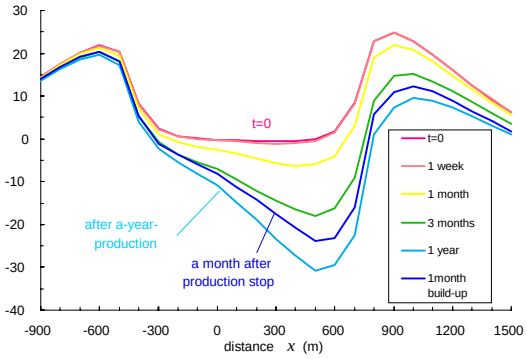


**Fig. 3 Simulated absolute SP profiles.**

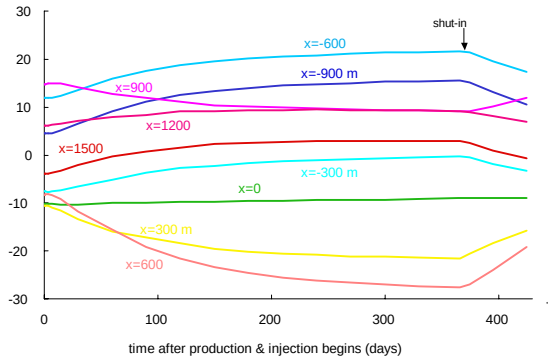


**Fig. 4 Simulated change of relative SP.**

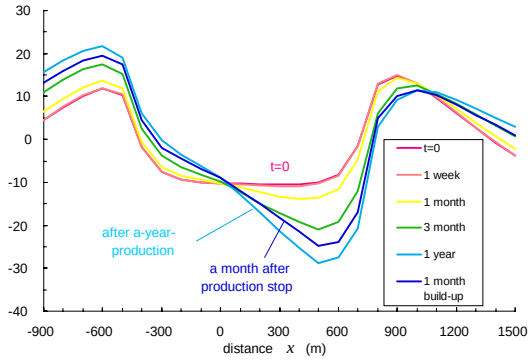


**Fig. 5 Relative SP profiles calculated for 25 observation points.**

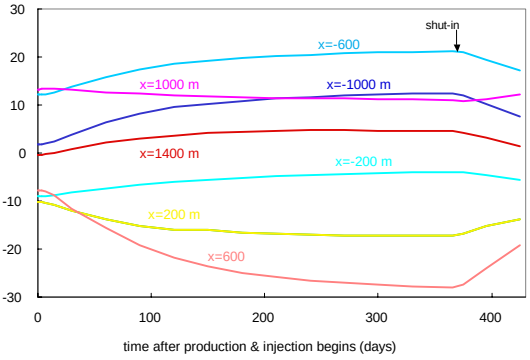


**Fig. 6 Simulated relative SP change for 7 observation points.**

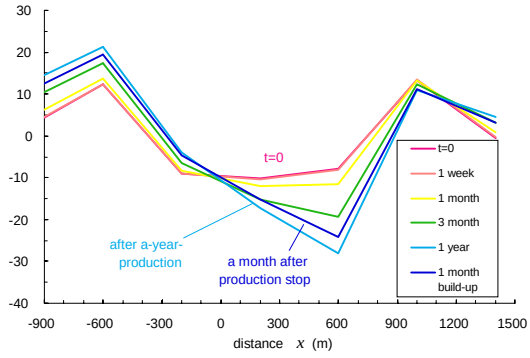


**Fig. 7 Relative SP profiles calculated for 7 observation points**

### 2.3 Desirable coverage area and spacing of SP monitoring points

To apply the relative SP technique, the number of observation points must be sufficient to cover the "target area". In a typical case, an area of diameter ~5d (where d is the depth of SP source) should be covered. Figs. 6 and 7 show the simulated relative SP change for the same case as Figs. 4 and 5 with seven observation points. As shown in these figures, relative SP is still useful for fewer observation points, if the points are distributed over the whole target area with equal spacing. However, the number of observation points must be large enough to avoid a problem of spatial aliasing. In the present case, the minimum number is six because the wave number in Fig.5 is 1.5. Large number is also desirable to get a good average value with high S/N.

## 3. SP MONITORING AT MORI

### 3.1 Mori geothermal field

Mori geothermal field is located in the Nigorikawa Basin, Hokkaido, Japan (Fig. 8). This basin is composed of a small Crater Lake type caldera with a diameter of 3 km (Kurozumi and Doi, 2002). Inside the caldera is filled by Quaternary sediments, identified as low resistivity zone by

Kajiwara et al. (1995), while outside the caldera is consists of Tertiary rocks. The basin is generally flat in topography, with elevations around 110 m above sea level.

An active hydrothermal system is identified at the northern part of the caldera wall. The geothermal reservoir in the caldera is a liquid-dominated system and hot spring discharges are identified in the northern part of the basin.

In this area, Japan Metals and Chemicals Co., Ltd. (JMC) and Dohnan Geothermal Energy Co., Ltd. (DGE) had done an extensive geothermal exploration since 1972 resulting in operation of Mori geothermal power plant since 1982 with installed capacity of 50 MW. Currently about 84 percent of produced fluid is injected from injection wells. The production level is 500 – 2000 m deep in the north-eastern part of the production zone shown in Fig. 9, while in the south-western part is 2000–3100 m. Injection level is 1300-1900 m deep in the south-western injection zone and 100-1300 m deep in the others, respectively.

### 3.2 SP monitoring at Mori

A continuous surface SP monitoring was conducted from July 31 to October 10, 2000, aiming to detect the change of subsurface fluid flow system caused by reservoir operation such as shut-in and re-opening of the wells. All production and injection wells were shut-in for a month from August 3 for annual maintenance of Mori geothermal power plant. The eight SP monitoring points are approximately aligning from west to east located inside the caldera over the reservoir region except for D5 to the east.

Figs. 10 (a) to (d) show the change of 24-hour-averaged relative SP at each observation point and rainfalls in the Nigorikawa basin. Vertical lines show the times of shut-in and re-start of the wells.

G12 and A8 in Fig. 10 (a), both located at the center of the basin near injection and production zones, show similar characteristics; SP decreases after shut-in and increases after re-opening. Clear negative responses immediately after rainfalls are identified since the effect of rain may be simple vertical infiltration at these points. In Fig. 10 (b), SP at E4, located in the middle of production zone, drastically increases around re-opening of the wells, though this change might be partly triggered by rainfall. These three points are marked as △ in fig. 9.

G7 and D in Fig. 10 (d) have opposite characteristics; SP increases during shut-in and decreases after re-opening. Positive responses to rainfall are detectable for D but not for G7. They are marked as ▲ in Fig. 9. E9 and S5 in Fig. 10 (c), both located near the edge of the basin, show similar characteristic as G7 and D, but the change is smaller and the effect of rain is unclear. They are marked as ◮ in Fig. 9.

SP at D5, located outside the basin marked as ○ in Fig. 9, has no clear response to the well operations (Fig. 10 (d)), suggesting that the reservoir region is limited inside the basin. At D5, significant high-frequency drift, probably amplified by high near-surface resistivity, is observed.

### 3.3 Discussions

The SP observation points at the Mori geothermal field are characterized from hydrological viewpoint.

G12 and A8, where SP decreases after shut-in and increasing after re-opening, are characterized as inside the production zone and/or outside the injection zone. This result is quite consistent with the fact that these points are located near both production and injection zones but the injection level is shallower. Since the influenced area by a shallower source is smaller than that by a deeper source, these points are under the influence of production but outside the influence of injection. As a result, these observation points show the characteristics of inside the production zone and outside the injection zone. Larger SP change at A8 than at G12 may be due to the shorter distance to the operation wells. Though larger SP change is often related to a higher near surface resistivity, it is not for this case because the electrical resistivity is equally low inside the caldera (Kajiwara et al, 1995).

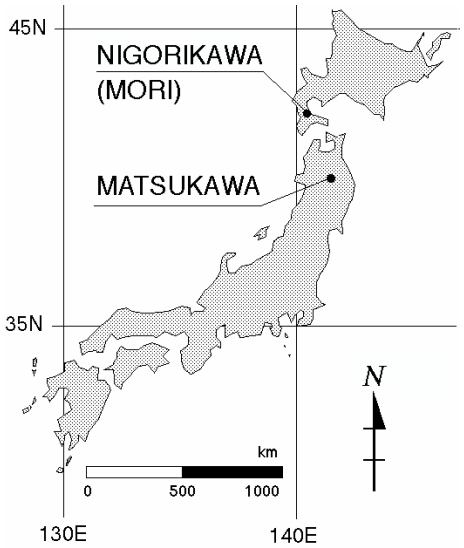


**Fig. 8 Locations of Mori and Matukawa geothermal fields.**

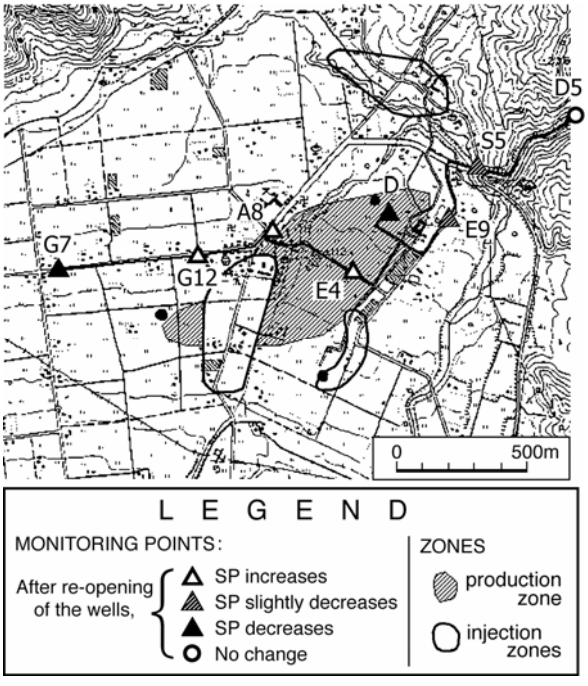


**Fig. 9 Location of SP monitoring points in Mori**

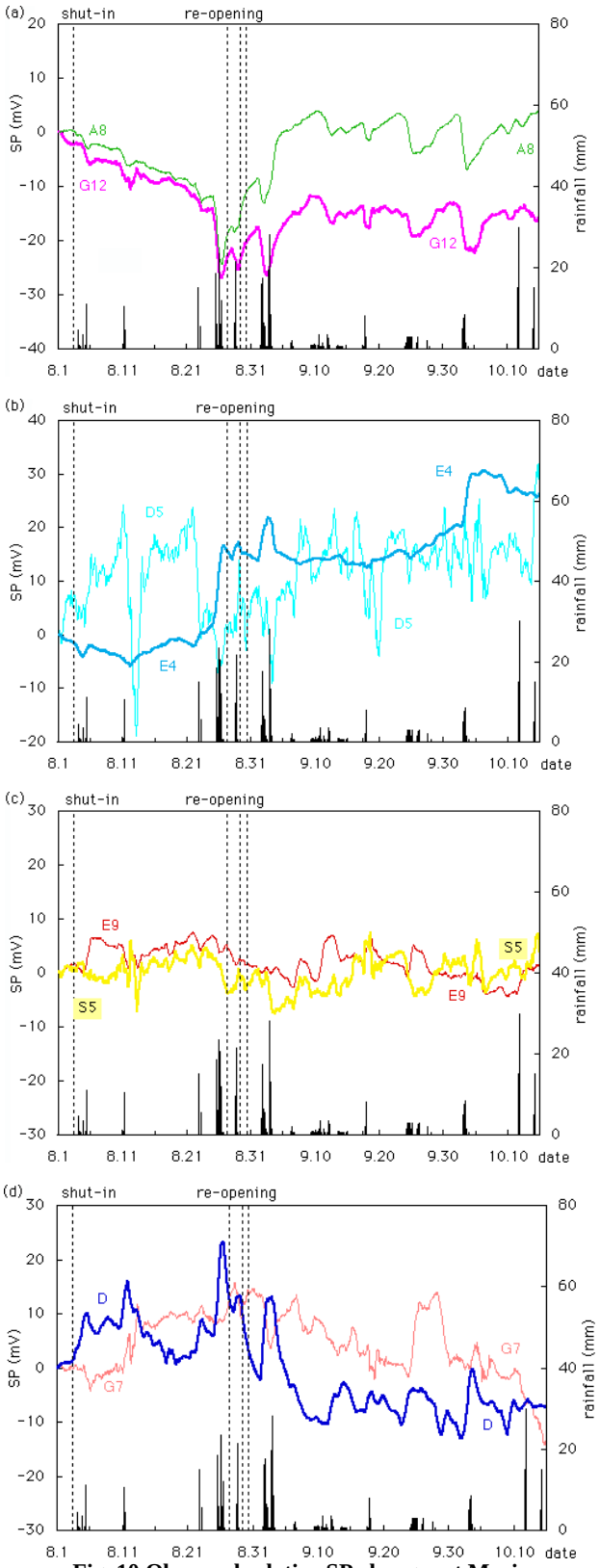


**Fig. 10 Observed relative SP changes at Mori:**

**(a) SP at G12 and A8, at the center of the basin, (b) SP at E4 and D5, (c) SP at E9 and S5, near the edge of the basin, (d) SP at D and G7**

SP at G7, D, E9 and S5 increases after shut-in and decreases after re-opening. This behavior is characterized as outside the production zone. Though G7 is outside both injection and production zones, since the total amount of production is larger, the effect of production is dominant on G7, characterizing it as outside the production zone. E9 and S5 are located near but outside the production zone. Although D is located inside production zone in rough scale, its behavior is that of outside the production zone, which may show that D is locally outside the production zone.

The drastic SP change at E4, which is located in the center of production zone, around re-opening of the wells might be caused by fluid production. Since its change is considerably faster than the others, its mechanism should be analysed by further studies, considering the effect of two-phase zones as well as the effect of localized rainfall. For E4, there is another drastic SP change in October for which the reason is not clear.

SP at D5, located outside the basin, has no clear response to the well operations. It suggests that the reservoir region is limited inside the basin. A considerably large high-frequency noise observed at D5 may be due to the higher resistivity of the shallow ground. According to the resistivity model by Kajiwara et al. (1995), based on the results of electro-magnetic methods, north-eastern outside the basin has higher resistivity at elevation of –300 to 1100 m above see level than inside the basin.

The effect of rainfall on SP is sharp and its duration is shorter in the central part of the basin, such as G12, A8 and E4 while the duration is longer near the edge of the basin, such as S5 and E9. It may be because shallow lateral flow from the outer basin prolongs the vertical infiltration near the border of the basin while vertical infiltration finishes soon after rainfall stops at the central part.

## 4. REPEAT SP SURVEY AT MATSUKAWA

### 4.1 The Matsukawa geothermal area

The Matukawa geothermal field is located in the Hachimantai volcanic region in northeastern Honshu, Japan (Fig. 8). The elevation of this field is about 850-1000 m above sea level. In this area, geothermal exploration had been initiated since 1952 and JMC has started power generation since 1966 as the first geothermal power station in Japan, succeeded by Tohoku Hydro and Geothermal Energy Co., Ltd. (TOHGEC) in 2003. Currently this system has the characteristics of a vapor-dominated reservoir, although it had two-phase zones at the beginning of fluid production. Water injection has been examined at intervals since 1988 to support reservoir pressure and to maintain steam production (Hanano, 2003). The effect of injection has been evaluated through several monitoring methods including tracer tests.

The Quaternary Matsukawa Andesite is widely exposed to the surface of the field. The geothermal reservoir consists of the Quaternary Andesite, the Pliocine to Pleistocine Welded Tuffs, the Miocine Formations and the diorite porphyry. The reservoir is seated along the Akagawa river from central to southwestern part of the field, while to the northeast is along the Matsukawa river (Fig. 11). The depths of the production zones of the wells are 700 to 1500 m.

### 4.2 SP survey at Matsukawa

SP surveys in Matsukawa were conducted as follows:

1st survey; 27 May – 29 May, 2002
2nd survey; 17 June – 18 June, 2002
3rd survey; 9 July, 2002
Shut-in of the wells; 6 June – 28 June

The first survey was conducted before the shut-in of the wells. The second and third surveys are about 10 days after shut-in and opening of the wells, respectively. Note that not all

production wells were shut-in during this period but only M-14, M-7, M-13, M-6, M-15 and M-9 were shut-in while the others were continuously open as shown in Fig. 11. Reinjection from MR-1, for which tracer returns are identified at wells M-12 and M-1, continued over the period at a flow rate of 15 – 30 tons/hour. The SP survey points are shown in Fig. 11. Central to southeastern points were not measured at the third survey because of the bad weather.

Fig. 12 shows the change of SP distribution before and after the shut-in of the wells ($SP_{June}$-$SP_{May}$). Red closed areas show the zones of positive SP change, where successive two or more survey points indicate positive change higher than 5 mV. The blue shadowed areas are the zones of negative SP change in the same manner as the positive ones. These positive and negative SP change zones are approximately aligned in NE-SW direction along Matsukawa and Akagawa rivers, where the major reservoir is located. Near the shut-in wells M-14, M-13 and M-15, negative zones appear. Negative and positive zones appear around well MR-1, into which injection was continued over the period.

Fig. 13 shows the change of SP distribution after re-opening of the wells ($SP_{July}$-$SP_{May}$). Compared to Fig. 12, the negative zone around the injection well MR-1 shrinks and the positive zones emerge into one. Also at the southwestern part, negative zones around M-14 almost disappear and a positive zone appears.

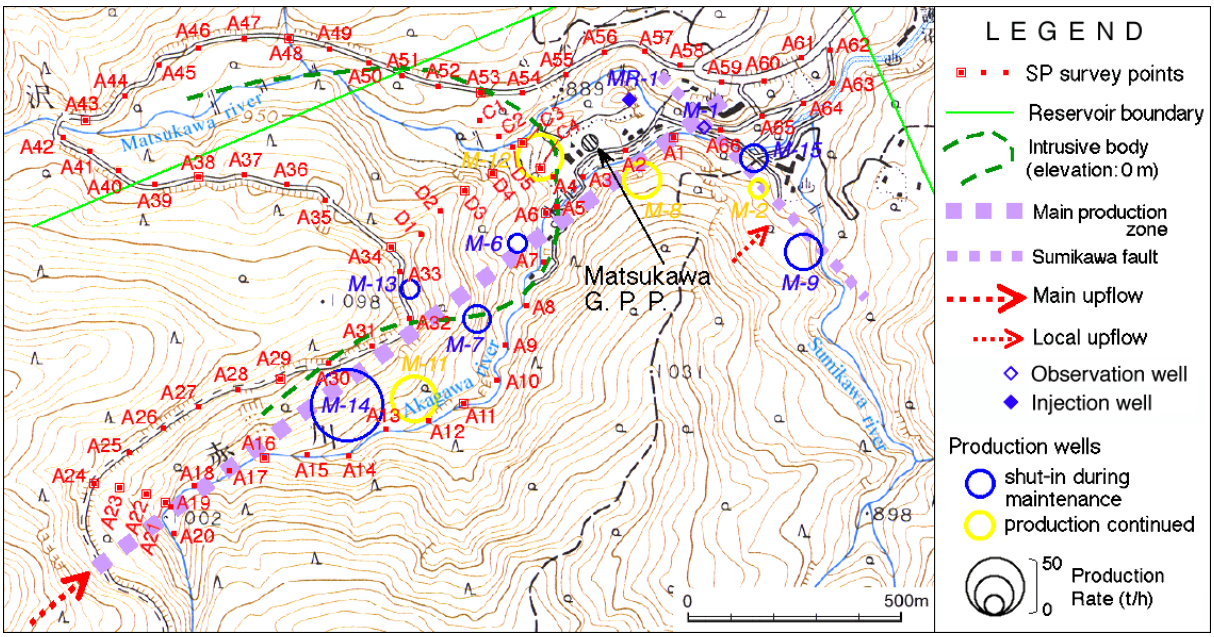


**Fig. 11 Map of SP survey points at Matsukawa. The reservoir boundary is suggested by Ozeki et al. (2000).**

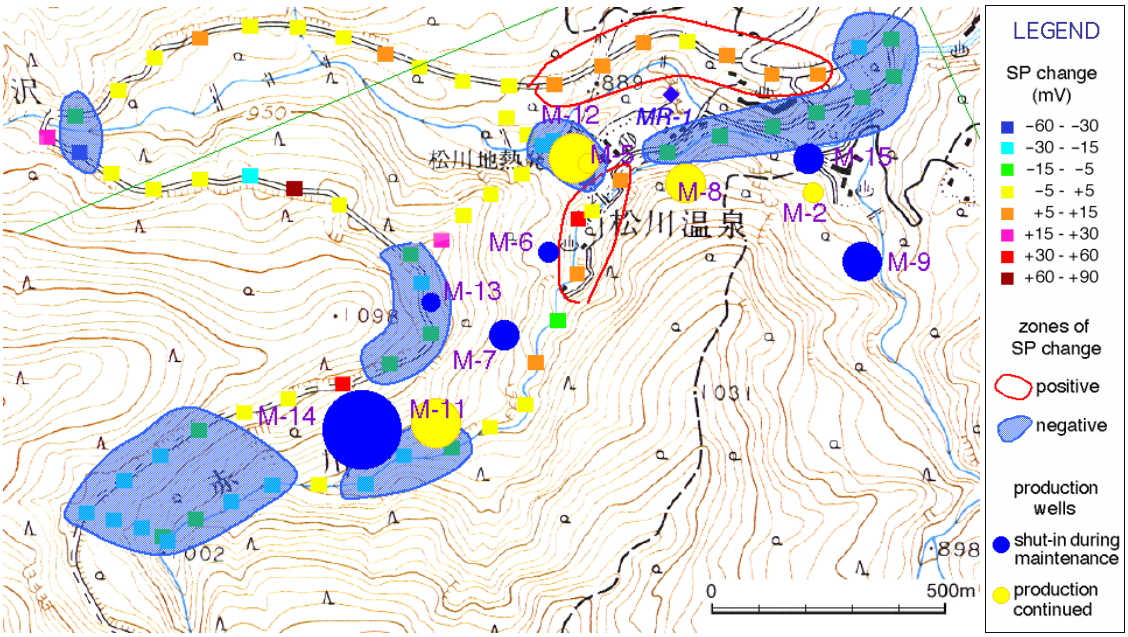


**Fig. 12 The change of SP distribution before and after the shut-in of the wells (June - May)**

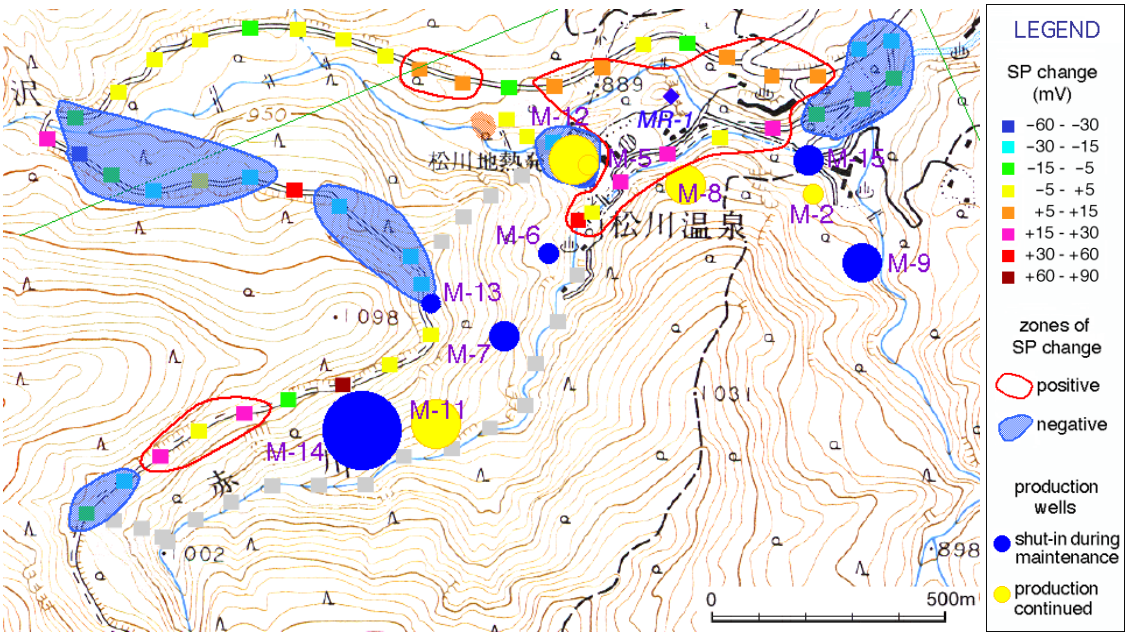


**Fig. 13 The change of SP distribution before shut-in and after the opening of the wells (July - May)**

### 4.3 Discussion

After shut-in of the wells, shown in Fig. 12, negative SP changes were observed at the surroundings of shut-in wells M-14, M-13, and M-15. It can be interpreted that the subsurface pressure increase after shut-in pushed down the liquid phase, which causes negative streaming potential at the surroundings, a few hundred meters from the well. This phenomenon is quite clear in case of M-14 because its regular production rate is highest (70 tons/hour) and it is located in the southwestern end so that the interference from the other wells is small.

After re-opening of the wells, shown in Fig. 13, positive SP changes were observed near M-14 and M-15. It may be the opposite phenomenon as the case of shut-in described above: pressure drop around the well pulls up the water level, which causes positive streaming potential. It is interesting that negative SP change was widely observed at the central to northwestern part. It may not be the effect of re-opening of the wells; but possibly the effect of shut-in of wells M-14, M-13, M-7 and M-6 slowly traveled to this zone by this time, 30 days after shut-in. Thus this zone may have a weak hydrological connection with the main reservoir.The mechanism of positive SP changes observed around MR-1 is not quite clear because there are interferences of many production wells and a injection well. In addition, since streaming potential appears as a result of combination of both vertical and horizontal flows (Yasukawa et al., 2003), the mechanism explained above, which is based on vertical flows only, must be too simplified. The resistivity structure and phase change are also important factors for SP data interpretation. For more detailed interpretation, numerical modeling with proper physical parameters is essential.

Nevertheless, part of the observed data shows the result that seems reasonable to explain by the simplified mechanism of streaming potential. The fact that distinctive SP changes were observed at several zones of the reservoir range is also an important result of this study. It shows that some liquid phase still exist in the reservoir, which is consistent with Hanano et al. (1991), which describes the condensation in the reservoir. The result also suggests that SP monitoring can be applied to steam dominated reservoirs as well as liquid dominated reservoirs

In view of some of uncertainties in relating SP to field production/injection, such as difference of rainfall effect on observation points due to topography, noise from solar activities, repeat survey under different conditions or continuous SP monitoring may give better idea for the interpretation.

## 5. CONCLUSIONS

A numerical modelling and a case study of SP monitoring are shown in this paper. Long term “relative” SP monitoring gives the hydrological characteristics of each observation point.

A repeat SP surveys conducted at the Matsukawa geothermal field, a steam dominated geothermal reservoir shows a result of distinctive SP changes from 5 to 30 mV at several zones. It suggests that liquid phase still exists in the reservoir and SP monitoring can be applied also to steam dominated reservoirs. A wider monitoring area may give the information about the reservoir boundary. For more detailed interpretation, numerical modeling with proper physical parameters is essential.

## ACKNOWLEDGEMENTS

The field observation in Mori and Matsukawa had been done through a cooperation project between JMC and AIST. The authors highly appreciate the contribution of JMC to the project especially during the field works at Matsukawa. The authors are also grateful to TOHGEC for giving permission to submit this paper with field data.

## REFERENCES

Goldstein, N. E., Halfman. S., Corwin, R. F. and Alvarez, J. R., 1989. Self-potential anomaly changes at the East Mesa and Cerro Prieto geothermal fields. Proceedings of the 14th workshop on geothermal reservoir engineering, Stanford University, p. 145-153.

Hanano, M., Sakagawa, Y. and Saida, T., 1991. Pressure build-up behavior of M-7 a dry steam well in Matsukawa, Japan. Journal of the Geothermal Research Society of Japan, v. 13, p. 45-53.

Hanano, M., 2003. Sustainable steam production in the Matsukawa geothermal field, Japan. *Geothermics*, v. 32, p. 311-324.

Ishido, T., Mizutani, H., 1981. Experimental and theoretical basis of electrokinetic phenomena in rock-water systems and its application to geophysics. *Journal Geophysical Research* **86**, 1763-1775.

Ishido T., Pritchett, J. W., 2000. Using numerical simulation of electrokinetic potentials in geothermal reservoir management, Proc., World Geothermal Congress 2000, **4**, 2629-2634.

Kajiwara, T., Mogi, T., Takahashi, M., Nishimura, S., Katsura, I., Suzuki, K., Kusunoki, K., Nishida, J., 1995. Geoelectrical Structure by CSMT and TDEM method at the Mori geothermal field, Hokkaido. *Proc., 93rd SEGJ Conference*, 181-185. (in Japanese)

Kurozumi, H. and Doi, N., 1994. An interpretation on the history of the Nigorikawa caldera. Abst., Soc. Volcano Japan, 1994 annual meeting, p.192. (in Japanese)

Matsushima, N., Kikuchi, T., Tosha, T., Nakao, S., Yano, Y., Ishido, T., Hatakeyama, K., Ariki, K., 2000. Repeat SP Measurements at the Sumikawa Geothermal Field, Japan, Proc., World Geothermal Congress 2000, **4**, 2725-2730.

Mitchell, J. K., 1993. Fundamentals of soil behavior, Wiley, New York.

Morrison, F., Corwin, R. F., De Moully, G., Durand, D., 1978. Interpretation of self-potential data from geothermal areas. Semi-annual technical report, Contract #14-08-0001-16546, Sponsored by U.S.G.S.

Nishino, T., Kainuma, N., Matsuyama, K., Muraoka, A., 2000. Self-potential survey in Hachijojima, Proc., World Geothermal Congress 2000, **4**, 2761-2766.

Ozeki, H., Fukuda, D. and Okumura, T., 2000. Recent study and geothermal model of the Matsukawa area, Japan. Proceedings of the Asia Geothermal Symposium 2000, p.94-103.

Revil, A., Pezard, P. A., Glover P. W., 1999. Streaming potential in porous media. 1. Theory of the zeta potential. *Journal Geophysical Research* **104** (B9), 20021-20031.

Tosha, T., Ishido, T., Matsushima, Y. and Nishi, U., 2000. Self-potential variation at the Yanaizu-Nishiyama geothermal field and its interpretation by the numerical simulation. Proceedings of the World Geothermal Congress 2000, v. 3, p. 1871-1876.

Yasukawa, K., Bodvarsson, G.S., Wilt, M. (1993). A coupled self-potential and mass-heat flow code for geothermal applications, *GRC Transactions*, Vol. 17, 203-207.

Yasukawa K., Suzuki I. and Ishido T., 2001. Reservoir monitoring by relative self-potential observation at the Nigorikawa Basin, Hokkaido, Japan. Geothermal Resources Council *Transactions*, v. 25, p. 705-710.

Yasukawa, K., Mogi, T., Widarto, D. and Ehara, S., 2003. Numerical modeling of a hydrothermal system around Waita volcano, Kyushu, Japan, based on resistivity and self-potential survey results. *Geothermics*, v. 32, p. 21-46.